

# A Virtual Exercise Machine

H. Kazerooni<sup>1</sup>, M. G. Her<sup>2</sup>

<sup>1</sup>Mechanical Engineering Department  
University of California at Berkeley  
Berkeley, CA 94720 USA

<sup>2</sup>Mechanical Engineering Department  
Tatung Institute of Technology  
Taipei, Taiwan, 104, R. O. C.

## ABSTRACT

This article discusses the dynamics and design of multiple-degree-of-freedom robotic systems built as general purpose exercise machines for the human arm. These machines may be programmed to give the human arm the sensation of forces associated with various arbitrary maneuvers. As examples, these machines can give the human the sensation that he/she is maneuvering a mass, or pushing onto a spring or a damper. In general, the machines may be programmed for any trajectory-dependent force. To illustrate and verify the analysis of these machines, a two-degree-of-freedom electrically-powered exercise machine was designed and built at the Motion Control Laboratory of the University of California-Berkeley.

## 1. MOTIVATION AND INTRODUCTION

This article describes the design and dynamics of powered general-purpose exercise machines. Figure 1 shows one example of such a machine: a two-degree-of-freedom exercise machine built at the University of California at Berkeley. This machine can be programmed to impose arbitrary trajectory-dependent forces on the human arm. The human maneuvers the machine in a vertical two-dimensional plane by holding a handle at the exercise machine endpoint. (More description on the experimental robot of Figure 1 is given in Section 5.)

Contrasting it with existing passive exercise machines makes clear the advantages of the active exercise machine discussed in this paper. The main advantage of this general-purpose powered active exercise machine is its flexibility: it can be programmed to give the human arm a sensation of various desired forces (i.e., resistance) over various arbitrary trajectories. Existing passive exercise machines do not offer such flexibility in their dynamic behavior. For example, existing weight machines can only produce constant forces (i.e., gravity) for the

users, and users must change steel disks to change the machine's resistance. Also, existing weight machines cannot produce behaviors similar to those of a spring or a damper. To get such behaviors one must use another exercise machine. Consider another example of a passive system: a rowing machine. The user rotates a flywheel by pulling two ropes; the forces imposed on the user's arms are function of the flywheel inertia and acceleration. This machine cannot impose constant forces on the human. The user has to change to a weight machine if constant forces are preferred.

The general-purpose powered active exercise machine discussed in this article lets the user choose a variety of forces over various trajectories. For example, the machine can be programmed to give the human the sensation that he/she is maneuvering a mass, or pushing onto a spring or onto a damper. There is no physical weight, damper or spring in the active machine; the entire dynamic behavior of the machine is created by the computer. The machine's computer creates a virtual dynamic behavior for the user.

Three elements contribute to the dynamics of these systems: the human, the exercise machine and the load being maneuvered. (Including the load may not seem mandatory in the design of such exercise machines at this point. However, as will be clarified later, the installation of a load and the direct measurement of the load force on the machine allow for the development of a more general class of performance for these machines.) The motion commands to the exercise machine are taken directly from two sets of interaction forces: one between the human and the machine, and one between the load and the machine. While the human interaction force helps move the exercise machine, the load interaction force impedes the machine motion.

---

\* This research is supported by a grant from NSF under contract number BCS-9196183.

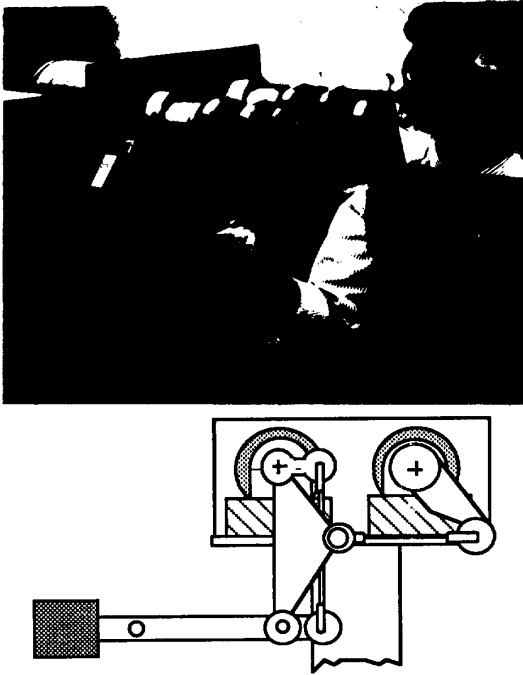


Figure 1: The two-degree-of-freedom general purpose exercise machine built at the University of California, Berkeley. The human maneuvers the machine in a vertical two-dimensional plane by holding a handle at the exercise machine endpoint.

## 2. DYNAMICS

This section describes the dynamic behavior of the exercise machine and the human arm, which are combined in Figure 2.

It is assumed that the exercise machine primarily has a closed-loop position controller, which is called the *primary stabilizing controller*. The resulting closed-loop system is called the *primary closed-loop system*. Exact dynamic models for the exercise machine are difficult to produce because of uncertainties in the dynamics of the machine actuators, transmissions and structure. These uncertainties become a major barrier to the achievement of the desired machine performance, especially when human dynamics are coupled with the machine dynamics in actual machine maneuvers. The exercise machine's primary stabilizing controller minimizes the uncertainties in the machine dynamics and creates a more definite and linear dynamic model for the machine. This linear model may then be used to design other controllers that operate on forces  $f_h$  (human force) and  $f_e$  (load force). For the experimental machine employed in this research

effort, the computed-torque method along with a PD controller [1, 2, 14] is used as the primary stabilizing controller to create a more definite and linear dynamics for the machine.

Regardless of the type of primary stabilizing controller, the exercise machine position,  $p$ , results from two inputs: 1) the desired position command,  $p_{des}$ , and 2) the forces imposed on the exercise machine. The transfer function matrix  $G$  represents the primary closed-loop position system which maps  $p_{des}$  to the machine position,  $p$ . Two forces are imposed on the machine:  $f_h$  is imposed by the human, and  $f_e$  is imposed by the load.  $S_h$ , an exercise machine sensitivity transfer function, maps the human force,  $f_h$ , onto the machine position,  $p$ . Similarly,  $S_e$ , an exercise machine sensitivity transfer function, maps the load force,  $f_e$ , onto the machine position,  $p$ . If the primary stabilizing controller is designed so that  $S_h$  and  $S_e$  are small, the exercise machine has only a small response to the imposed forces  $f_h$  and  $f_e$ . A high gain controller in the primary stabilizing controller results in small  $S_h$  and  $S_e$  and consequently a small machine response to  $f_h$  and  $f_e$ . Using  $G$ ,  $S_e$  and  $S_h$ , equation 1 represents the dynamic behavior of the exercise machine.

$$p = G p_{des} + S_h f_h + S_e f_e \quad (1)$$

The middle part of the block diagram in Figure 2 represents the exercise machine model (i.e., equation 1) interacting with the human and the load. The upper left part of the block diagram represents the human dynamics. The human arm's force on the exercise machine,  $f_h$ , is a function of both the human muscle forces,  $u_h$ , and the position of the machine,  $p$ . Thus, the machine's motion may be considered to be a position disturbance occurring on the force-controlled human arm. If the machine is stationary (i.e.,  $p = 0$ ), then the force imposed on the machine is solely a function of the human muscle force command produced by the central nervous system. Conversely, if the exercise machine is in motion and  $u_h = 0$ , then the force imposed on the machine is solely a function of the human arm impedance,  $H(p)$ .  $H$  is a nonlinear operator representing the human arm impedance as a function of the human arm configuration;  $H$  is determined primarily by the physical properties of the human arm [7, 8, 13, 15]. Based on the above, equation 2 represents a dynamic model of the human arm.

$$f_h = u_h - H(p) \quad (2)$$

The specific form of  $u_h$  is not known other than it results from human muscle force on the exercise machine [4, 5].

It is assumed that the exercise machine is maneuvering a small load. The load force impedes the machine motion. The exercise machine controller translates the two measured interaction forces into a motion command for the machine to create a desired relationship between the human forces and the load forces.  $E$  is a nonlinear operator representing the load dynamics.  $f_{ext}$  is the equivalent of all the external forces imposed on the load which do not depend on  $p$  and other system variables. Equation 3 provides a general expression for the force imposed on the exercise machine,  $f_e$ , as a function of  $p$ .

$$f_e = -E(p) + f_{ext} \quad (3)$$

In the example of accelerating a point mass  $m$  along a horizontal line, the load force,  $f_e$ , can be characterized by  $f_e = ms^2 p$ . In this case  $E = ms^2$  and  $f_{ext} = 0$  where  $p$  is the mass position and  $s$  is the Laplace operator. If the load is large and cannot be represented by a point mass, then  $E$  can be calculated using Lagrangian formulation.

The diagram of Figure 2 includes two linear controllers,  $\alpha(s)$  and  $K(s)$ , which modulate the forces  $f_h$  and  $f_e$ .  $\alpha$  and  $K$  (which are implemented on a computer) must be designed to produce a desired performance in the exercise machine system.

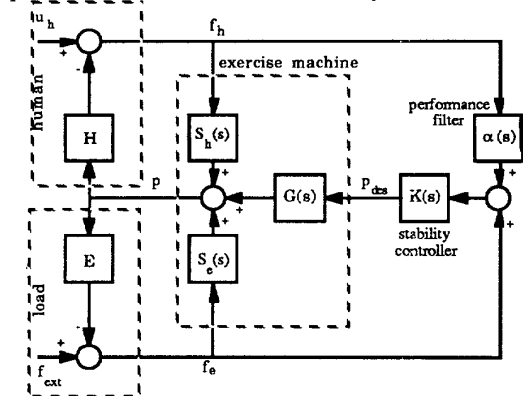


Figure 2: The overall block diagram for the exercise machine. The machine dynamics, which are linearized by the primary stabilizing controller, are represented by  $G$ ,  $S_h$  and  $S_e$ . The human and the load dynamics are represented by two nonlinear operators  $H$  and  $E$ . Two linear controllers  $\alpha$  and  $K$  modulate the forces  $f_h$  and  $f_e$ .

### 3. CONTROL

To understand the role of controllers  $\alpha$  and  $K$ , assume for a moment that neither controller is included in the system. If the commanded position,  $p_{des}$ , the

human muscle forces,  $u_h$ , and the external forces,  $f_{ext}$ , all equal zero, then the exercise machine position,  $p$ , equals zero, and no motion is transmitted to the load. This is the case when the human is holding the exercise machine without intending to maneuver it. If the human decides to initiate a maneuver, then  $u_h$  takes on a nonzero value, and an exercise machine motion develops from  $f_h$ . The resulting motion is small if  $S_h$  is small. In other words, the human may not have enough strength to overcome the exercise machine's primary closed-loop controller.

To increase the human's effective strength, the exercise machine's effective sensitivity to  $f_h$  must be increased by measuring the human force,  $f_h$ , and passing it through the controllers  $\alpha$  and  $K$ . Figure 2 shows that  $GK\alpha$ , parallel with  $S_h$ , increases the effective sensitivity of the machine to  $f_h$ .  $K$  and  $\alpha$  must be chosen to ensure the stability and performance of the closed-loop exercise machine system.

Next, the following question is addressed: how should the exercise machine perform in a particular maneuver? The following example illustrates a simple specification for the exercise machine performance. The human uses the machine to maneuver a free mass in space. A reasonable performance specification for this example would state the level of amplification of the human force which is applied to the free mass. If the force amplification is large, a small force applied by the human results in a large force being applied to the free mass. If the amplification is small, a small force applied by the human results in a small force being applied to the free mass. Consequently, if the amplification is large, the human "feels" only a small percentage of the interaction force with the free mass. Most importantly, the human still retains a sensation of the dynamic characteristics of the free mass, yet the load essentially "feels" lighter or heavier as exercise required.

With these heuristic ideas of system performance, the exercise machine performance is captured in equation 4 where  $f_h^*$  is the human force applied to maneuver the machine when no load is present.  $R$  is the performance matrix, and  $[0, \omega_p]$  is the frequency range of the human arm motion.

$$(f_h - f_h^*) = -R f_e \quad \text{for all } \omega \in [0, \omega_p] \quad (4)$$

Equality 4 guarantees that  $(f_h - f_h^*)$ , the portion of the human force that is actually applied to maneuver the load, is proportional to the load force,  $f_e$ . The performance matrix  $R$  is an  $n \times n$  linear transfer function matrix. Suppose  $R$  is chosen as a diagonal matrix with all members having magnitudes smaller than unity over some bounded frequency range. Then the human force is smaller than the load force by a factor of  $R$ . Suppose

R is chosen as a diagonal matrix with all members having magnitudes greater than unity. Then the human force is larger than the load force by a factor of R. In a more complex example, the transfer function matrix R may be selected to represent linear passive dynamic systems.

By inspecting Figure 2, the exercise machine position is written as a function of  $f_h$  and  $f_e$ .

$$p = (G K \alpha + S_h) f_h + (G K + S_e) f_e \quad (5)$$

Now suppose that the human maneuvers the exercise machine through the same trajectory indicated by p in equation 5 except without any load. The no-load human force,  $f_h^*$ , is then obtained by inspection of Figure 2 where  $E = 0$  and  $f_{ext} = 0$ :

$$p = (G K \alpha + S_h) f_h^* \quad (6)$$

Equating the trajectories from equations 5 and 6 results in equation 7.

$$(f_h - f_h^*) = - (G K \alpha + S_h)^{-1} (G K + S_e) f_e \quad (7)$$

Comparing equations 4 and 7 shows that to guarantee the performance represented by R in equation 4, inequality 8 must be satisfied.

$$\sigma_{\max} [(G K \alpha + S_h)^{-1} (G K + S_e) - R] < \epsilon \quad (8)$$

for all  $\omega \in [0, \omega_p]$

where  $\sigma_{\max}$  represents the maximum singular value.  $\epsilon$  represents a small positive number chosen by the designer to denote the degree of precision required for the specified performance within the frequencies  $[0, \omega_p]$ . A small value for  $\epsilon$  (e.g., 0.01) indicates a close proximity of the actual system performance to the specified performance R (e.g., within a 1% error). Note that the human and load dynamics, H and E, are absent from inequality 8. Thus, achievement of the specified performance R depends only on the exercise machine dynamic behavior (G,  $S_e$ ,  $S_h$ ) and on the controllers (K,  $\alpha$ ), and not on the particular human operator and load. Assuming that R is selected so  $R^{-1}$  always exists,  $\alpha$  is chosen to be equal to  $R^{-1}$ . Substituting  $R^{-1}$  for  $\alpha$  in inequality 8 shows that any K which satisfies inequality 9 also satisfies 8.

$$\sigma_{\max} (GK) > \frac{\sigma_{\max} (S_e - S_h R) \sigma_{\max} (R)}{\epsilon} \quad (9)$$

for all  $\omega \in [0, \omega_p]$

Inequality 9 suggests that, since  $\epsilon$  is a small number, the designer must choose K to be a transfer function matrix with large magnitude to satisfy inequality 9 for frequencies  $\omega \in [0, \omega_p]$  and for a given  $\epsilon$ , R,  $S_h$  and  $S_e$ . The smaller  $\epsilon$  is chosen to be, the larger K must be to achieve the desired performance. K

may not be arbitrarily very large: the choice of K must also guarantee the closed-loop stability of the system shown in Figure 2, as discussed in the next section.

#### 4. STABILITY

The selection of K is particularly important since H and E generally contain nonlinear dynamic components. The following questions illuminate our approach to the design of K. In designing K, is it possible to work with a human and a load with linear dynamics (represented by  $H_0$  and  $E_0$ ) instead of the nonlinear dynamics represented by operators H and E? If the answer is yes, then what properties should  $H_0$  and  $E_0$  have so that the designed K both satisfies inequality 9 and stabilizes the Figure 2 system in the presence of a family of nonlinear operators H and E?

The block diagram of Figure 2 is transformed into the block diagram of Figure 3 in order to group the nonlinear operators, H and E, into one block on the diagram.

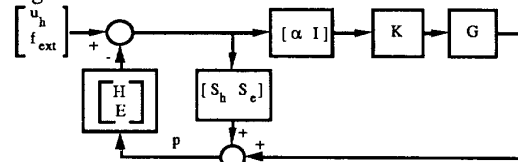


Figure 3: Simplified block diagram of Figure 2. I is a unity matrix.

$S_h$  and  $S_e$  represent the sensitivities of the exercise machine position to the human and load forces. G,  $S_h$  and  $S_e$  depend on the nature of the machine's primary stabilizing controller. If a primary stabilizing controller with a large position loop-gain or integral control is chosen to insure small steady state errors, then  $S_h$  and  $S_e$  are extremely small compared to G, approaching zero at steady-state. Prototype exercise machine designs have produced sensitivities on the order of  $10^3$  to  $10^6$  times smaller than G [9, 10]. Therefore  $S_h$  and  $S_e$  are disregarded in the following stability analysis. Figure 4 presents the resulting simplified stability diagram.

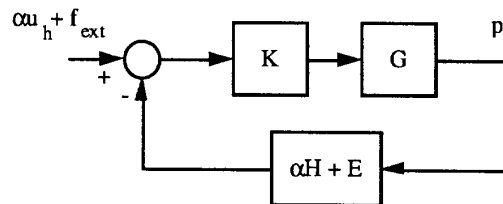


Figure 4: In systems with very small sensitivity transfer functions,  $S_e$  and  $S_h$  are much smaller than G and their effect on the overall system dynamics is negligible.

If  $H_0$  and  $E_0$  are assumed to represent a particular set of linear human and load dynamics, equation 10 represents the general form of  $H$  and  $E$  where  $\Delta$  is the stable nonlinear part of the dynamics.

$$\alpha H(p) + E(p) = [\alpha H_0 + E_0] p + \Delta(p) \quad (10)$$

Note that  $[\alpha H_0 + E_0]$  is a transfer function matrix operating on  $p$ . The block diagram of Figure 4 can be transformed into the block diagram of Figure 5.

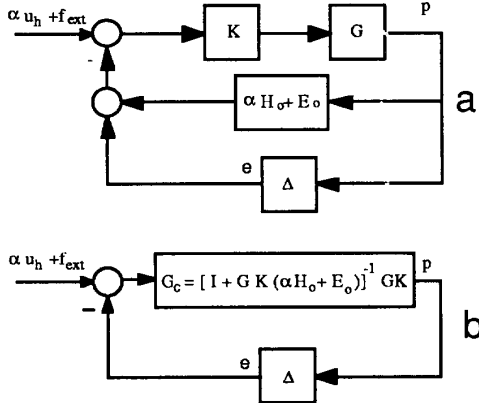


Figure 5:  $\Delta$  is the stable nonlinear operator representing the nonlinear human and load dynamics.

With respect to Figure 5, the design of  $K$  is approached as follows. A stabilizing controller  $K$  must be designed for a set of linear  $H_0$  and  $E_0$  so that the closed-loop system of Figure 5 remains stable and inequality 9 (indicating the performance) is satisfied. This controller must guarantee enough stability robustness for all bounded values of  $H$  and  $E$ . Therefore the goal is to find a particular class of  $H_0$  and  $E_0$  and a stabilizing controller  $K$  that together yield the largest stability robustness for a given largest  $\Delta$ . Equation 11 represents the forward loop in Figure 5b.

$$G_c = [I + GK(\alpha H_0 + E_0)]^{-1} GK \quad (11)$$

The stability of each element in Figure 5b is described by inequalities 12, 13 and 14:

$$\|\alpha u_h + f_{ext}\|_{\infty} \leq \beta_{in} < \infty$$

"input is  $L_{\infty}$  bounded" (12)

$$\|e\|_{\infty} \leq \lambda_{\Delta} \|p\|_{\infty} + \beta_{\Delta}$$

" $\Delta$  is  $L_{\infty}$  stable" (13)

$$\|p\|_{\infty} \leq \lambda_{G_c} \|e\|_{\infty} + \beta_{G_c}$$

" $G_c$  is  $L_{\infty}$  stable" (14)

$\lambda$  and  $\beta$  are finite positive constants that indicate  $L_{\infty}$  stable mappings. The closed-loop system of Figure 5 is  $L_{\infty}$  stable if the norm of the output  $p$  is bounded. According to the Small Gain Theorem [6], this is guaranteed if inequality 15 is satisfied.

$$\lambda_{G_c} \lambda_{\Delta} < 1 \quad (15)$$

The human arm impedance  $H$  changes from person to person and also within one person over time. This leads to large variations for  $\lambda_{\Delta}$ . To obtain an intuitive feel for the stability condition in inequality 15, evaluation of inequality 15 within the the operating range of the exercise machine system is useful. If  $K$  is designed as a very large transfer function in order to guarantee machine system performance (as prescribed by inequality 9), then equation 11, within the controller bandwidth, may be approximated by:

$$G_c \approx [\alpha H_0 + E_0]^{-1} \quad \text{for all } \omega \in [0, \omega_p] \quad (16)$$

One must choose the largest load that an exercise machine can manipulate to be  $E_0$ , the strongest human impedance to be  $H_0$ , and the greatest force amplification as a performance specification to be  $\alpha_{max}$ . Then,  $[\alpha_{max} H_0 + E_0]$  will be larger, and  $G_c$  and consequently  $\lambda_{G_c}$  will be smaller. If  $\lambda_{G_c}$  is smaller, then, according to inequality 15,  $\lambda_{\Delta}$  takes on larger values. In other words, if the largest values of  $\alpha$ ,  $H$  and  $E$  are used to design a stabilizing  $K$  (i.e., one that guarantees inequality 9), then the closed-loop system will remain stable in the presence of the large variations of human and load dynamics represented by a large  $\lambda_{\Delta}$ .

Inequality 9 also teaches that a large  $K$  is needed to guarantee achievement of the system performance. Inspection of Figure 4 shows that choosing a large  $[\alpha_{max} H_0 + E_0]$  for stability robustness (as discussed above) restricts the designer's choices for a large  $K$ . This is true because large values for both  $K$  and  $[\alpha_{max} H_0 + E_0]$  may cause a large loop gain and consequently an unstable system in Figure 4. Therefore, although choosing a large value for  $[\alpha_{max} H_0 + E_0]$  leads to stability robustness, it may prohibit the designer's choosing a large  $K$  to satisfy the performance specification in inequality 9. Thus, the better understood the load and human dynamics are, the smaller  $\lambda_{\Delta}$  will be; this leaves more room to increase  $K$  and gain more precision in achieving the desired performance as stated by inequality 9. Similar stability analysis is given for robotic compliant maneuvers and force control systems [11, 12].

## 5. EXPERIMENTAL ANALYSIS

### Exercise Machine

The prototype two-degree-of-freedom electric direct-drive exercise machine (Figure 1 and Figure 6) is used to verify experimentally the theoretical predictions of the machine's stability and performance.

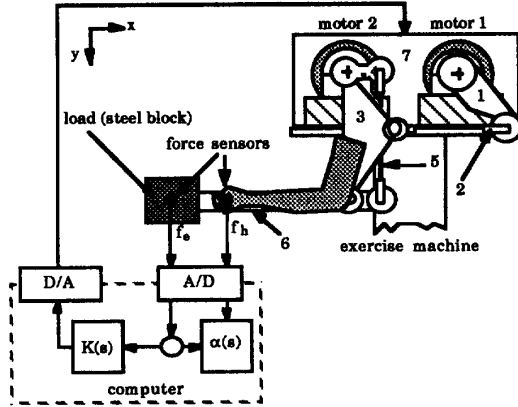


Figure 6: The experimental exercise machine used to verify the analysis.

Figure 6 shows the seven-bar-linkage mechanism used for our prototype laboratory exercise machine. This machine has two degrees of freedom corresponding to a shoulder and an elbow. Force sensors are mounted at the human-machine and machine-load interfaces. Motor 2 rotates link 4 causing the main arm (link 6) to move up and down via a four-bar linkage (links 4, 5, 6, and 3 as the ground link). In another four-bar linkage (links 1, 2, 3, and 7), motor 1 rotates link 1 causing the follower link (link 3) and the main arm (link 6) to move in and out. Both motors 1 and 2 are connected to bracket 7 which is mounted on a platform at the same height as the human shoulder. A gripper is mounted on link 6 where the operator force,  $f_h$ , is measured along two directions. Each link is machined as one solid piece rather than as an assembly of smaller parts. Employing the primary controller, the exercise machine closed-loop transfer function  $G$  in the Cartesian coordinate frame along the  $x$ - and  $y$ -directions of Figure 6 is:

$$G(s) = \frac{1.2516s + 2.079}{0.002s^3 + s^2 + 1.2516s + 2.079} \quad \text{Newton/Newton} \quad (17)$$

### Human Arm

The human arm dynamics do not affect performance (defined by inequality 9) but do play a major role in exercise machine stability. Several experiments were conducted to measure the human arm impedance  $H$ . Then the largest of these impedances was

chosen to be  $H_0$  in the stability analysis. In the experiments to determine the largest  $H$ , the subject grasped a handle on the exercise machine. The machine was commanded to oscillate via sinusoidal functions. The frequency and amplitude of oscillation were changed continuously by the software. (See Reference [3] for more detailed information about the nature of these experiments.) The human operator tried to move his/her hand to follow the machine so that zero contact force would be maintained between the hand and the machine. The human arm, when trying to maintain zero contact forces on the handle, cannot keep up with the high-frequency motion of the exercise machine. At high frequencies, the forearm is moved without the benefit of active feedback from the central nervous system. In other words, in the high frequency region, we observe that the impedance behaves like a purely inertial load. Thus, large contact forces and consequently a large  $H$  are expected at high frequencies. Since this force is equal to the product of the exercise machine acceleration and human arm inertia (Newton's Second Law), at least a second-order transfer function is expected for  $H$  at high frequencies. At low frequencies (in particular at DC), the operator can follow the machine motion comfortably, and can establish almost constant contact forces between the hand and the exercise machine. Thus, small contact forces at all machine positions and consequently a constant transfer function for  $H$  are expected at low frequencies.

Figure 7 shows the experimental values and the fitted transfer functions for two different experiments. In the first experiment (shown by plus signs), the subject holds the machine handle loosely. In the second experiment (shown by squares), the subject holds the machine handle very tightly. At low frequencies, the human arm impedance is smaller when the subject holds the handle loosely than when the subject holds the handle very tightly. Observing the slope of 40 db/dec for both plots show an inertial behavior at high frequencies. The largest impedance (shown by squares) is chosen for use in the stability analysis.

$$H_0 = 12.1 \left( \frac{s^2}{43.69} + \frac{s}{5.08} + 1 \right) \text{ lbf/ft} \quad (18)$$

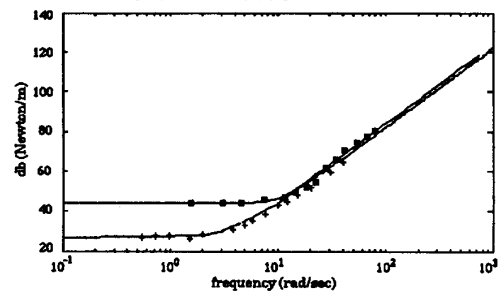


Figure 7 The Experimental and Theoretical Plot of  $H$ .

### Load

The mass that was installed on the exercise machine endpoint is 33.82 Newtons at a distance of 0.5 meter from the elbow joint as shown in Figure 6. The handle was mounted at 0.3 meter from the elbow joint. The equivalent of the heaviest load dynamics needed for stability analysis is represented by equation 19.

$$E_0 = 9.08s^2 \quad \text{newton/meter} \quad (19)$$

### Performance

Matrix R in equation 20 is chosen as the performance matrix in the Cartesian coordinate frame.

$$R^{-1} = \alpha = \begin{pmatrix} 8 & 0 \\ 0 & 5 \end{pmatrix} \quad (20)$$

The above performance specification has force amplifications of 8 times in the x-direction and 5 times in the y-direction. The human operator maneuvers the exercise machine irregularly (i.e., randomly). Figures 8 and 9 show  $f_e$  versus  $(f_h - f_h^*)$  along the x and y directions where the slope of -8 and -5 represent the force amplification by a factor of 8 and 5 along the x and y directions.

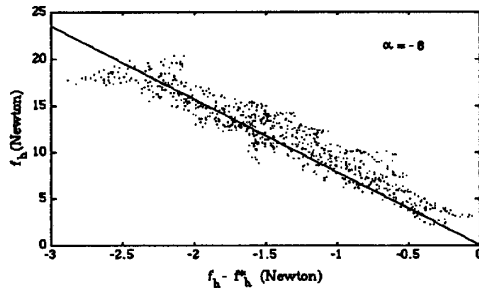


Figure 8:  $f_e$  versus  $(f_h - f_h^*)$  along the x-direction at  $\alpha = -8$ .

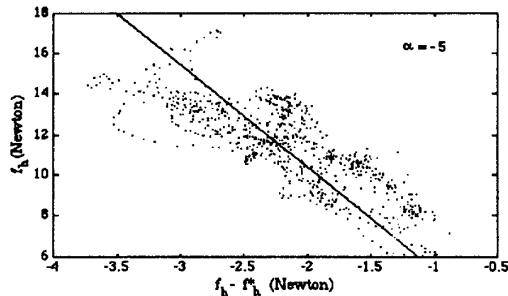


Figure 9:  $f_e$  versus  $(f_h - f_h^*)$  along the y-direction at  $\alpha = -5$ .

### 6. REFERENCES

1. An, Chae H., Atkeson, Christopher G., Hollerbach, John M., "Model-Based Control of Robot Manipulator", MIT Press, 1988.
2. Asada, H., Slotine, J. E., "Robot Analysis and Control", Wiley, New York, 1986.
3. Berthoz, A., Metral, S., "Behavior of Muscular Group Subjected to a Sinusoidal and Trapezoidal Variation of Force", J. of Applied Physiol., Volume 29, pp:378-384, 1970.
4. Cooke, J. D., "Dependence of human arm movements in limb mechanical properties", Brain Res., Volume 165, pp: 366-369, 1979.
5. Cooke, J. D., "The Organization of Simple, Skilled Movements", Tutorials in Motor Behavior, edited by G. Stelmach and J. Requin, Amsterdam, Elsevier, 1980.
6. Desoer, C. A., Vidyasagar, M., "Feedback Systems: Input-output Properties", Academic Press, 1975.
7. Feldman, A. G., "Functional tuning of the nervous system with control of movement or maintenance", J of Biophysics, V11, pp565-578.
8. Houk, J. C., "Neural control of muscle length and tension", in: Motor control, ed. V. B. Brooks. Bethesda, MD, American Physiological Society Handbook of Physiology.
9. Kazerooni, H., "Human-Robot Interaction via the Transfer of Power and Information Signals", IEEE Transactions on Systems and Cybernetics, Vol. 20, No. 2, Mar. 1990.
10. Kazerooni, H., Mahoney, S., "Dynamics and Control of Robotic Systems Worn By Humans", ASME Journal of Dynamic Systems, Measurement, and Control. Vol. 133, No. 3, September 1991.
11. Kazerooni, H., "On the Contact Instability of the Robots When Constrained by Rigid Environments," IEEE Trans. on Automatic Control, Vol. 35, No. 6, Jun. 1990.
12. Kazerooni, H., "On the Robot Compliant Motion Control", ASME Journal of Dyn. Systems, Measurement, and Control, Vol. 111, No. 3, Sept. 1989.
13. Marsden, C. D., Merton, P. A., Morton, H. B., "Stretch reflexes and servo actions in a variety of human muscles", Journal of Physiol., London, Volume 259, pp: 531-560.
14. Spong, M. W., Vidyasagar, M., "Robust Nonlinear Control of Robot Manipulators", Proc. 24th IEEE CDC, Ft. Lauderdale, FL, Dec. 1985.
15. Stein, R. B., "What muscles variables does the nervous system control in limb movements?", J. of the behavioral and brain sciences, 1982, Volume 5, pp 535-577.